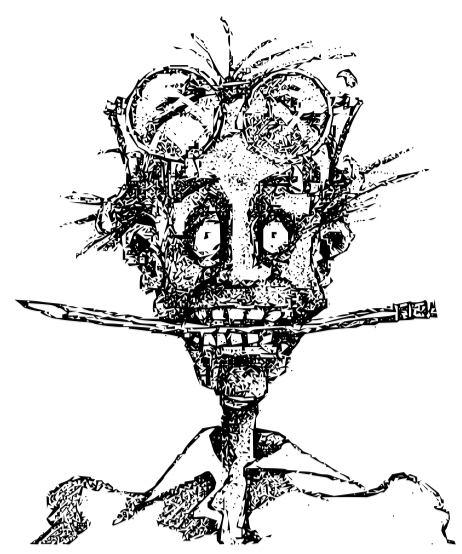


# Quantitative Prediction of Erythrocyte Sickling for Anti-Polymerization Activities in Sickle Cell Disease

L. Lu<sup>a</sup>, Z. Li<sup>a</sup>, H. Li<sup>a</sup>, X. Li<sup>a</sup>, P. Vekilov<sup>b</sup>, G. Karniadakis<sup>a</sup>

<sup>a</sup>Division of Applied Mathematics, Brown University

<sup>b</sup>Departments of Chemical and Biomolecular Engineering and Chemistry, University of Houston



BROWN

## Introduction

Sickle cell disease (SCD) originates from the mutation of a single nucleotide in the gene for hemoglobin. This mutation enables polymerization of sickle hemoglobin (HbS) molecules into polymers under hypoxia. Once a nucleus forms, HbS molecules rapidly associate to the nucleus, leading to fiber growth. The growing HbS fibers distort RBCs into a variety of shapes. The kinetic model to quantitatively predict RBC sickling:

- employs nucleation theory to explicitly describe the kinetics of homogeneous and heterogeneous nucleation of HbS monomers, as well as chemical rate laws to model the growth dynamics of HbS fibers;
- can predict the fraction of sickled RBCs according to the patient-specific inputs and organ-specific environmental conditions, and examine the therapeutic efficacy of anti-sickling agents.

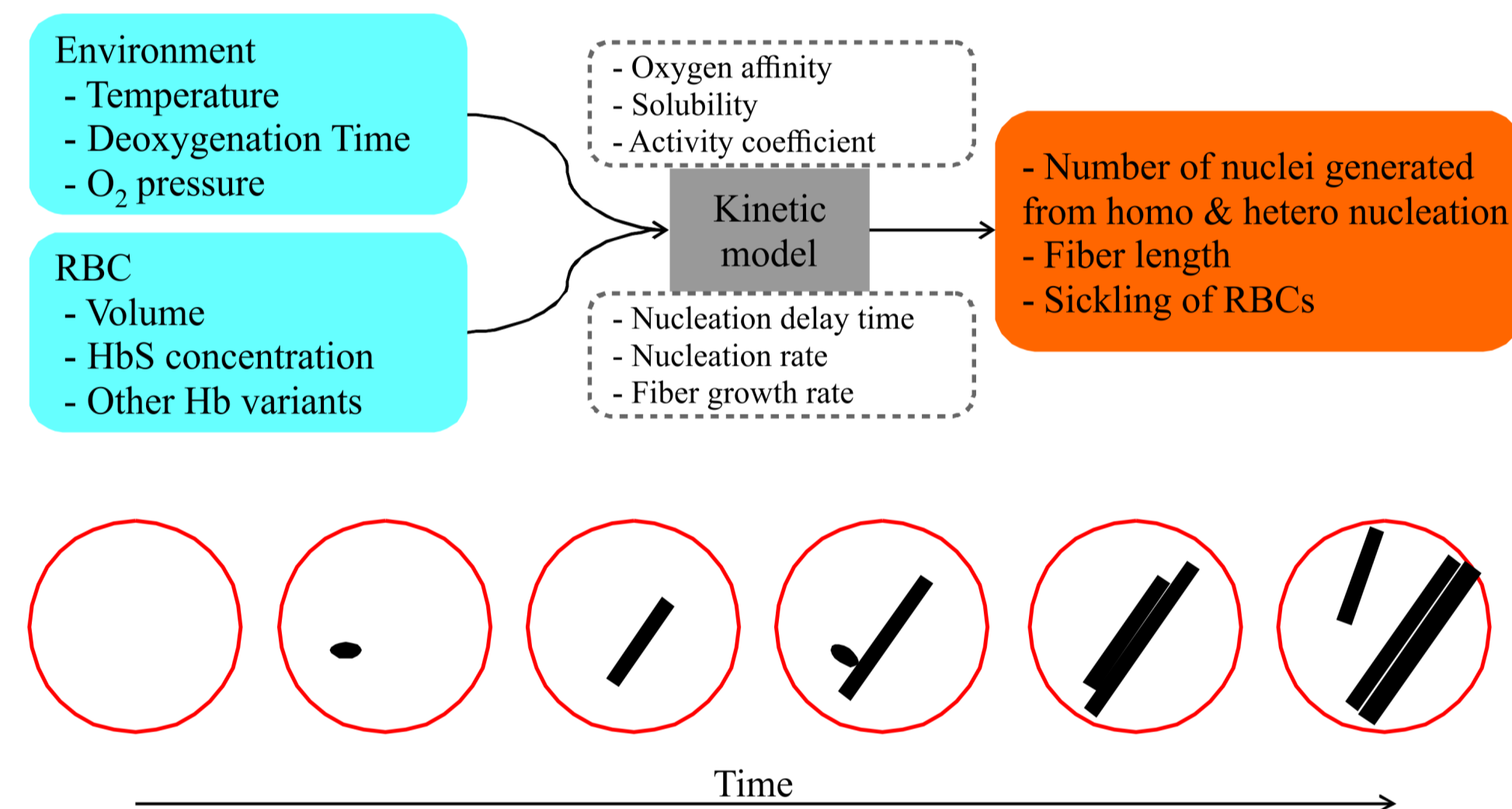


Figure 1: Schematic of the inputs and outputs of the kinetic model (upper), which describes the intracellular nucleation, growth and branching of HbS fibers and RBC sickling (lower).

## Mechanics of RBC sickling in SCD

Sickling of RBCs is induced by the growth of HbS fibers. We simulate the interaction between an RBC and HbS fibers.

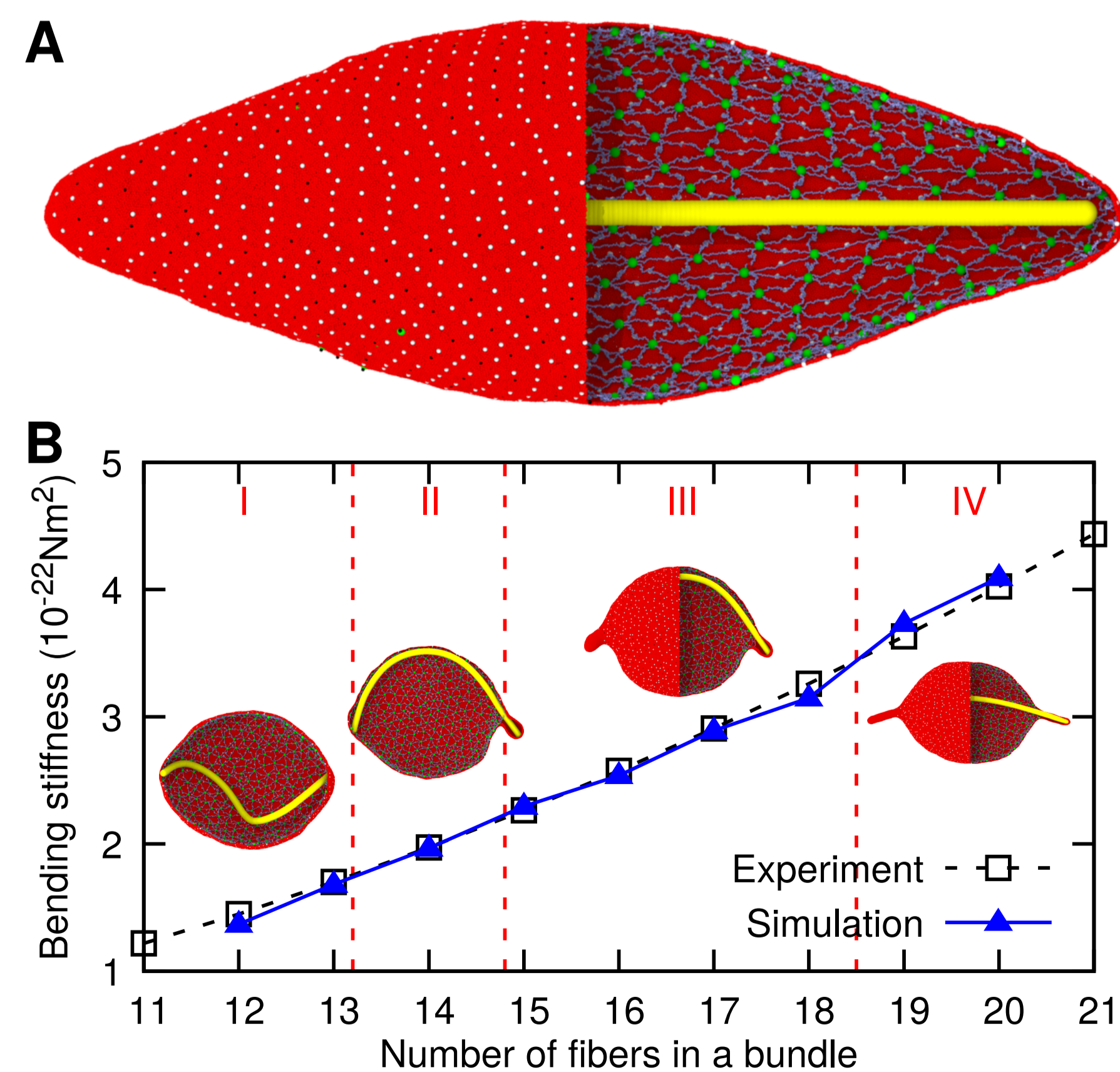
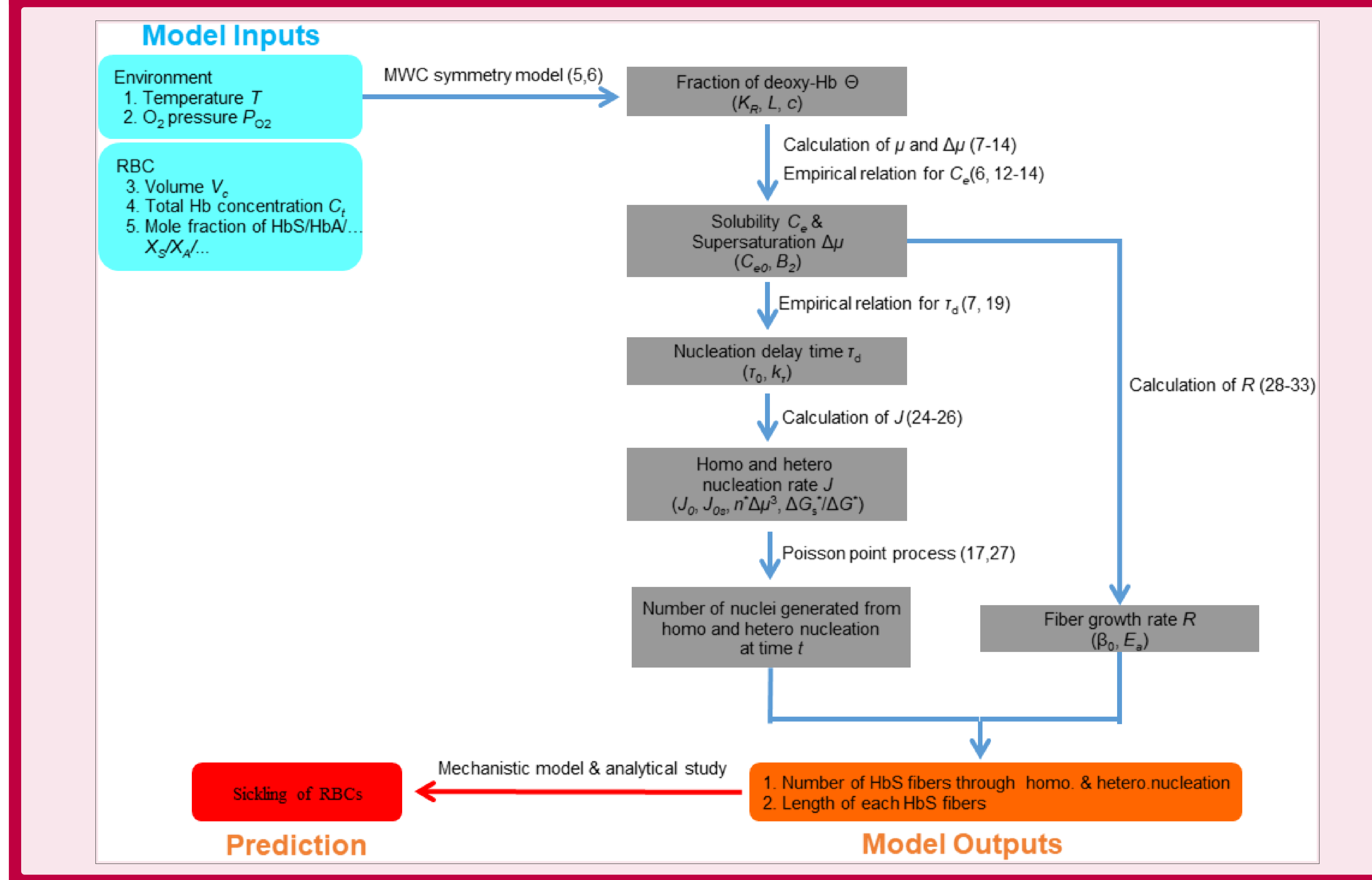


Figure 2: Simulations of RBC sickling with mechanistic models. (I) fiber buckled, (II) fiber buckled with one protrusion, (III) fiber buckled with two protrusions, (IV) non-buckled with two protrusions.

## Flow chart of prediction of RBC sickling through the kinetic model



## RBC sickling in the hepatic vein

To validate the model prediction of RBC sickling in hepatic vein, the simulation results are compared to experimental measurements.

- (A) The decrease of  $P_{O_2}$  from 100 mmHg to 28.1 mmHg in 1s enforces deoxygenation of hemoglobin from 4.3% to 49%.
- Fractions of RBCs of (B) sickle cell patient and (C) sickle trait individuals.

Sickling is more likely to occur for those RBCs with  $C_t > 34.3$  g/dl (area D), which accounts for  $\sim 24.3\%$  of RBCs. This result is close to the fraction of sickled RBCs (22%) observed in the hepatic vein of SCD patients.

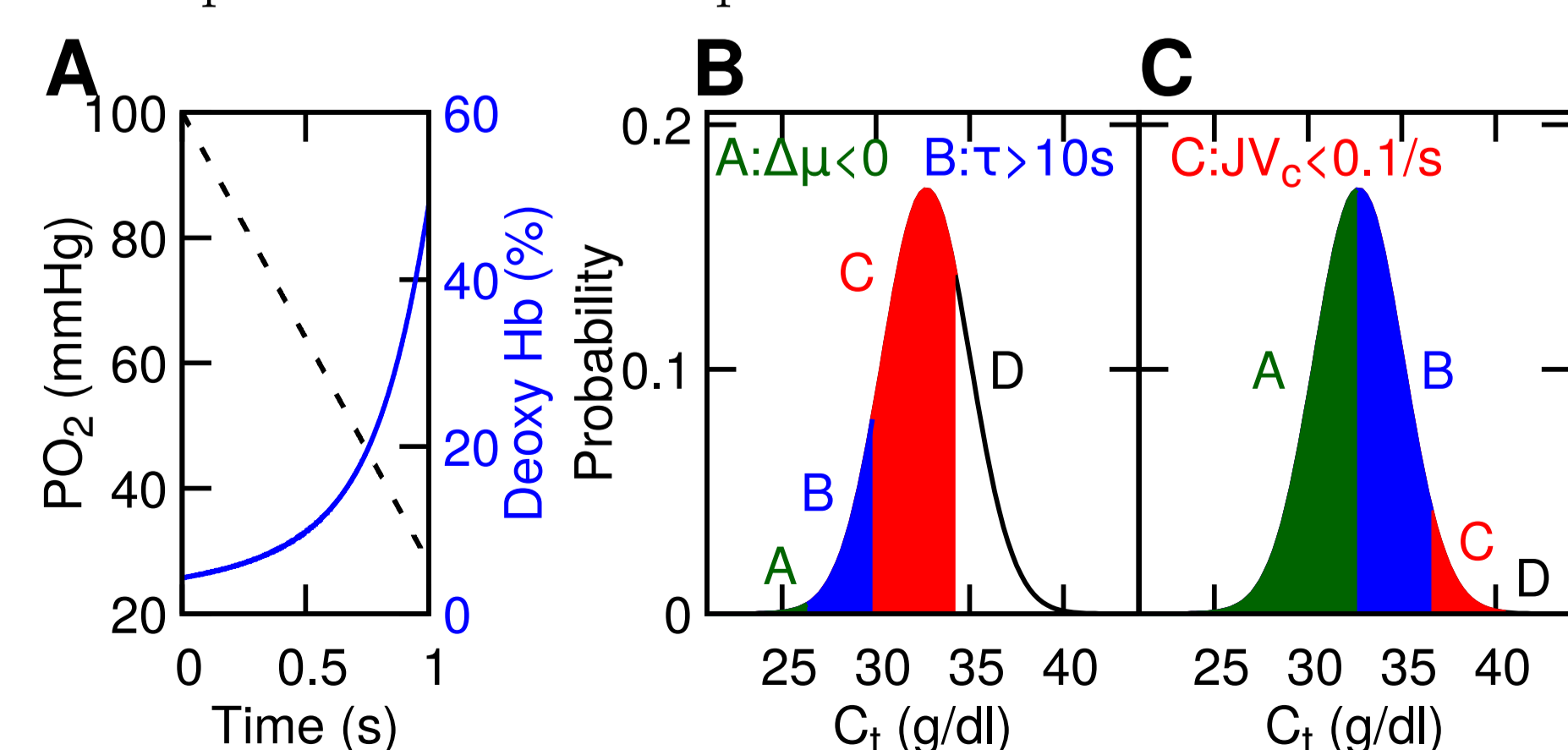


Figure 3: Deoxygenation and fraction of sickled RBCs in hepatic vein. Area A: Deoxy HbS is undersaturated. Area B: the nucleation delay time is longer than 10s. Area C: less than 1 polymer is generated via homogeneous nucleation within 10s. Area D: RBCs become sickled within 10s.

## Patient-specific studies of RBC sickling in microfluidic channel

We simulate fractions of sickled RBCs measured for seven SCD patients employing a microfluidics device. In this *in vitro* study,  $P_{O_2}$  in the microfluidic channel was reduced from 160 mmHg ( $O_2$  concentration of 21%) to 15.2–38 mmHg ( $O_2$  concentration of 2%–5%) in 15s.

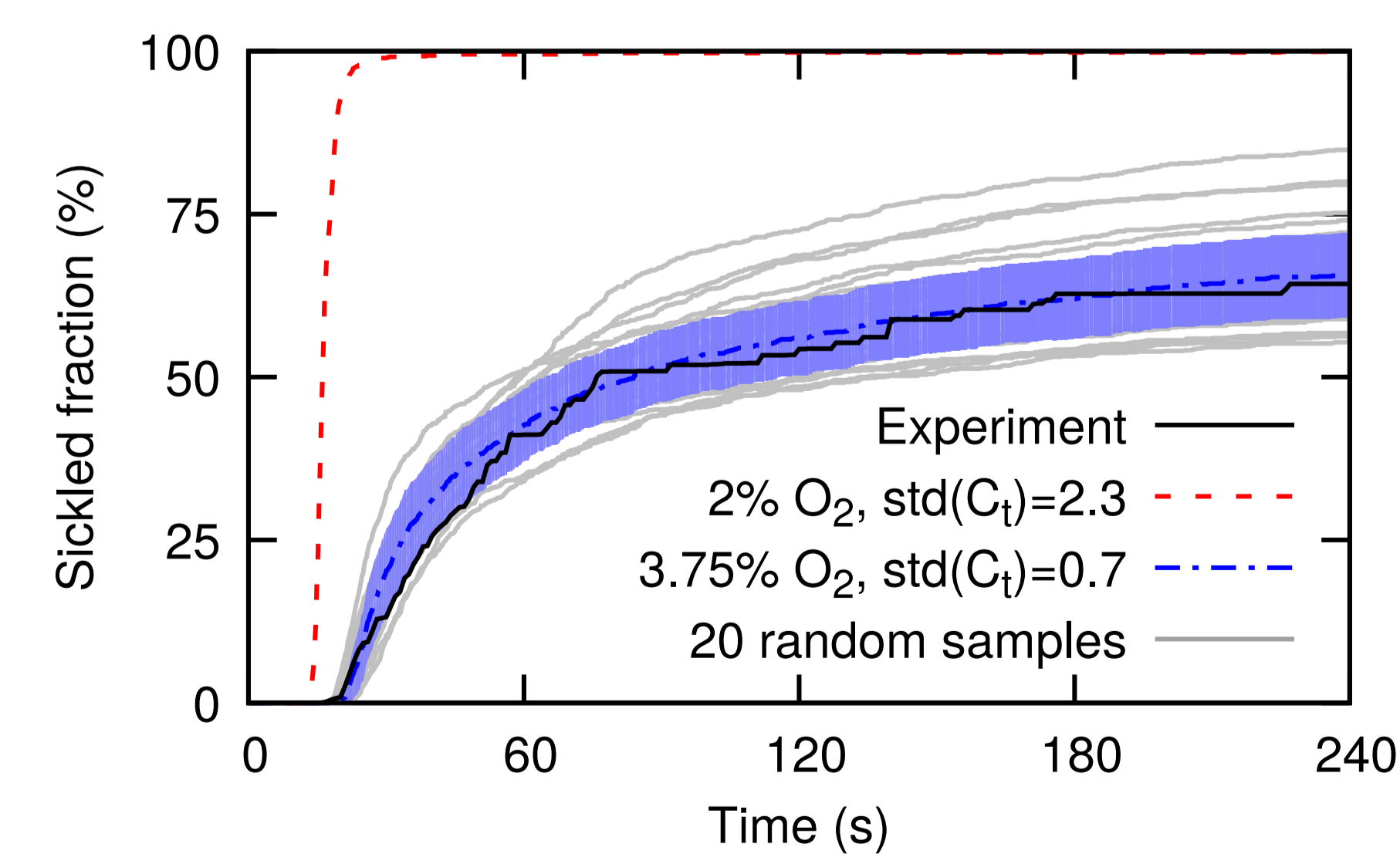


Figure 4: Evolution of fraction of sickled RBCs under hypoxia.

## Contact Information

Email: lu\_lu\_1@brown.edu

## Examination of sickling inhibitors

Monensin A and gramicidin A have demonstrated therapeutic effects by increasing cell volume. We apply our model to test this mechanism.

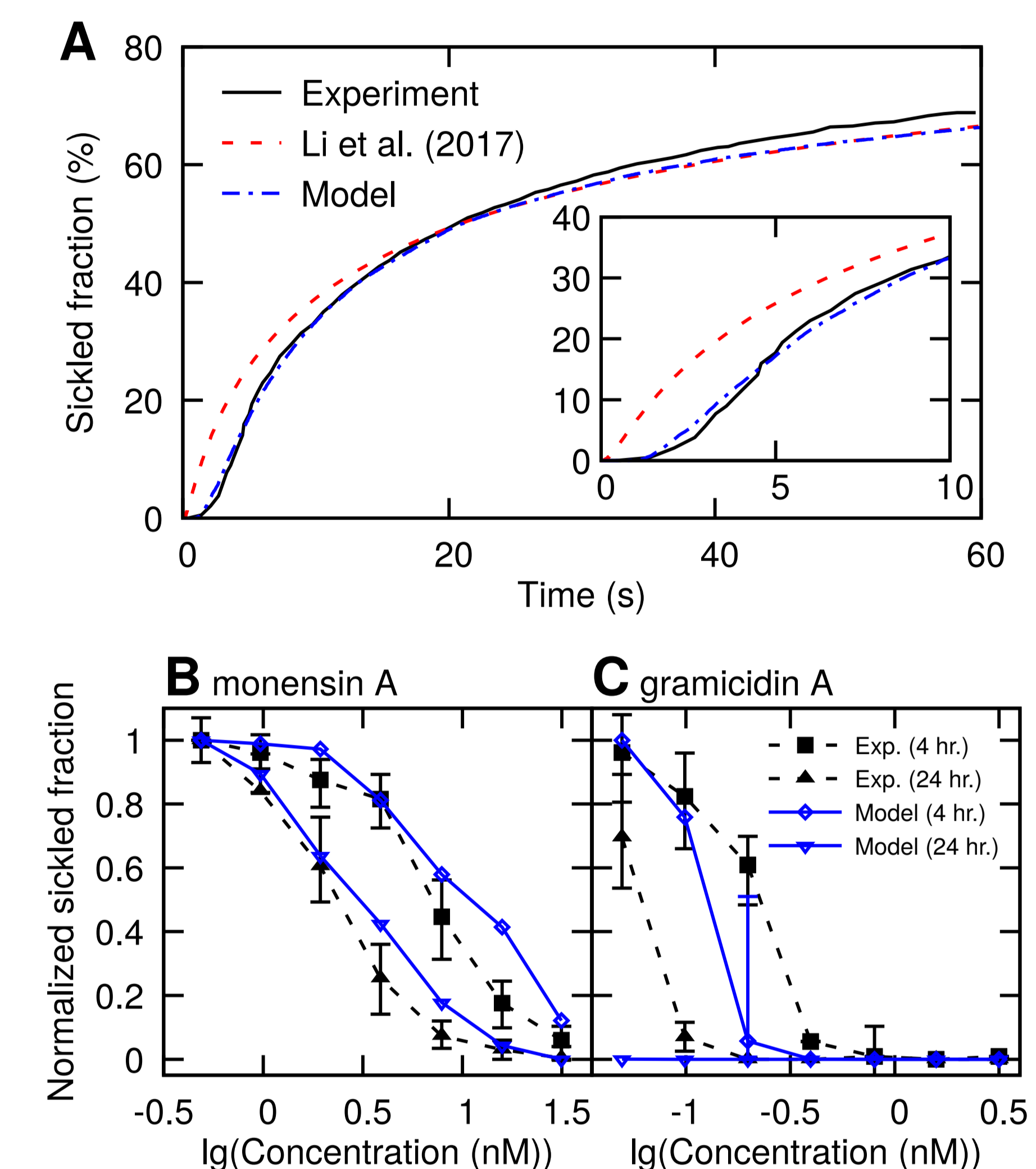


Figure 5: (A) Evolution of the fraction of sickled RBCs in the absence of sickling inhibitors. (B and C) The fraction of sickled RBCs decreases with increased MCV at 60 s after photolysis.

## Global parametric sensitivity analysis on the model parameters

The sensitivity of a single parameter is plotted as a circle, whose diameter reflects the sensitivity of the polymerization kinetics to that parameter. The connecting lines indicate the interaction of two parameters, which describes how the fraction of sickled RBCs changes when two parameters are varied synchronously.

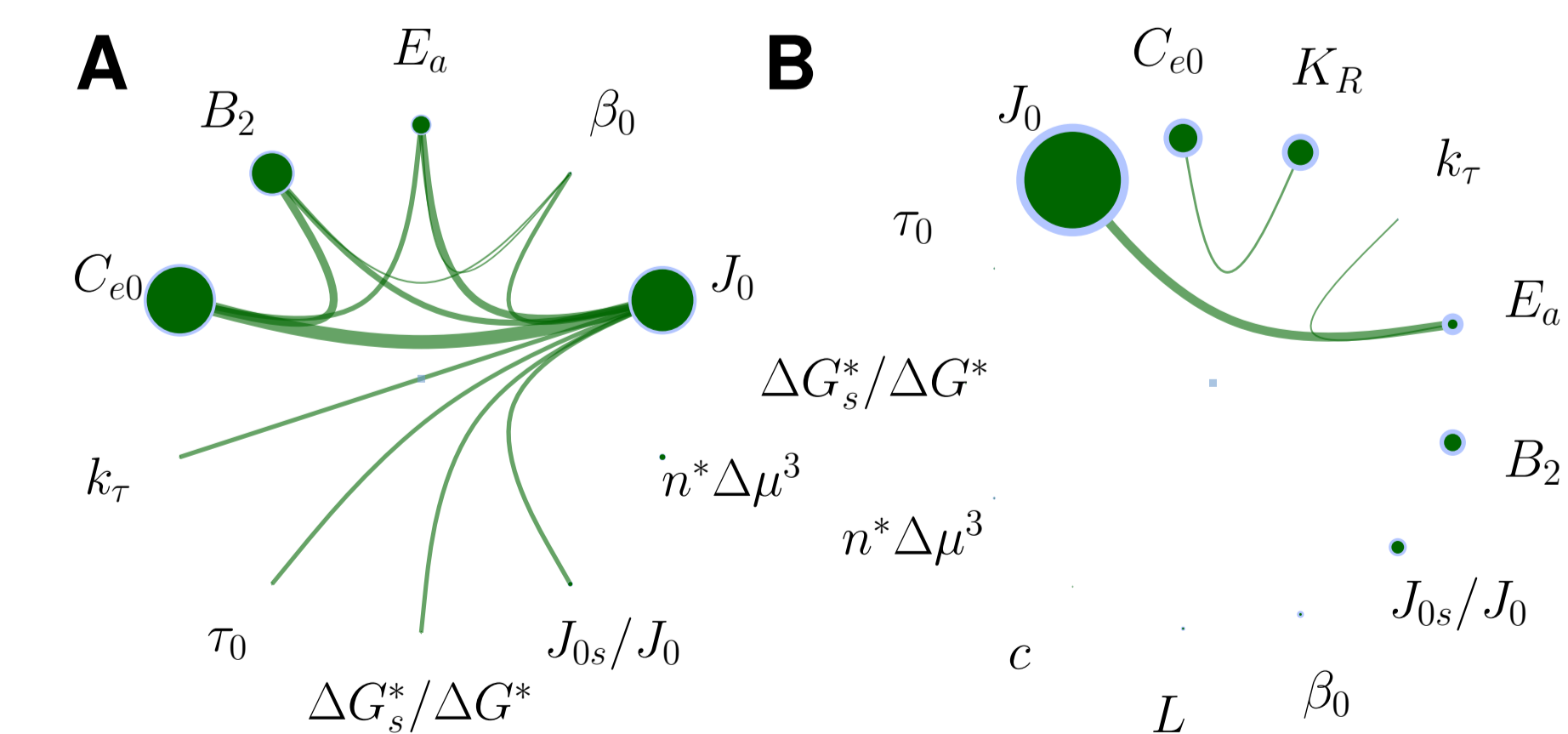


Figure 6: Sensitivity analysis with model inputs of an *in vitro* study (A) and an *in vivo* study (B).

## Acknowledgements

We would like to thank Dr. William A. Eaton for providing valuable suggestions, and Dr. E Du for providing the experimental data. The work was supported by NIH grants.